*Progress In Electromagnetics Research M, Vol. 64, 23–33, 2018*

# The Effect of Aspect Ratio and Fractal Dimension of the Boundary on the Performance of Fractal Shaped CP Microstrip Antenna

**Yagateela P. Rangaiah[1], R. V. S. Satyanarayana[2], and Pasumarthy N. Rao[1, *]**

**Abstract**—A simple single feed circularly polarized microstrip antenna with Koch curve as boundary is presented. The two pairs of rectangular microstrip antenna edges are replaced by a Koch curve of 1st stage and 2nd stage with different indentation angles to get circular polarization. The proposed method is simple and easy to obtain circular polarization with reasonable 3 dB axial ratio bandwidth and 10 dB impedance bandwidth. The dependency of aspect ratio and fractal dimension of the boundary on the performance of the circularly polarized antenna is discussed.

## 1. INTRODUCTION

Current communication and sensor systems require a high degree of polarization control to optimize system performance. For microstrip antennas to be fully functional in such systems, and high polarization purity and isolation between orthogonal polarizations are needed, while they may be linear or circular [1]. Fractals enable us to increase the length of a curve effectively in a given space. The systematic way of increasing the length of a fractal curve can be done with the help of fractal dimension, which is defined as the space filling ability of the curve. To obtain circular polarization, the antenna is to have different electrical lengths in the two perpendicular directions of the patch such that orthogonal degenerate modes are excited.

For all calculations involving circular polarization, the series combination of two parallel RLC circuits is used to model the resonant behavior of the single feed circularly polarized microstrip antenna. This arises from the fact that feed independently excites two orthogonal modes, each of which is modeled as a single RLC circuit. The total voltage at the feed location is the sum of the voltages due to the individual modal responses, hence the equivalent circuit is two RLC circuits in series [2].

There are many methods reported in the literature to introduce the asymmetry in the cavity of the patch [3–16]. The effect of fractal dimension on the resonant behavior of dipole antennas is presented by Vinoy et al. [17]. Rao and Yagateela [15] have reported circular polarization (CP) antenna with Koch curve as boundary to the triangular patch. However, it is easier to get CP with a rectangle-shaped antenna. Farswan et al. [18] reported a Koch CP antenna with a square patch. They used only one indentation angle, whereas the present paper discusses the effect of aspect ratio on the quality of circular polarization by changing indentation angle of the curve starting from 0 to 60°. In this paper regular geometry of the patch is perturbed in order to introduce asymmetry with the help of Koch fractal curve to get circular polarization. It is known that when a straight line of length '$L$' is transformed into a Koch fractal curve of iteration '$n$' with indentation angle '$\theta$', the effective length will be increased and is given by [16],

$$L_{\mathrm{n}} = \left(\frac{4}{2(1+\cos\theta)}\right)^{n} L \tag{1}$$

*Received 26 August 2017, Accepted 21 November 2017, Scheduled 19 January 2018*

* Corresponding author: Pasumarthy Nageswara Rao (nrraop@yahoo.com).

[1] Department of Electronics and Communication Engineering, Vardhaman College of Engineering, Hyderabad, India. [2] Department of ECE, S V U College of Engineering, Tirupati, India.

When the indentation angle is chosen as 60°, the length of the curve will be increased to $4/3*L$. Hence if the indentation angle of the boundary is chosen differently in two perpendicular directions of the patch, the required orthogonal modes will be generated resulting in circular polarization. Simultaneously the fractal dimension of the boundary also changes. The fractal dimension of Koch curve can be calculated using the formula given in Eq. (2).

$$D = -\frac{\log n}{\log \frac{1}{s}} \tag{2}$$

where $n$ = number of copies and $s$ = scaling factor.

For the standard Koch curve, indentation angle $(\theta) = 60°$, $n = 4$, $s = 3$ and $D = 1.261$. If the indentation angle is made variable, the scaling factor becomes function of $\theta$ and is given by

$$\frac{1}{s} = \frac{1}{2(1 + \cos\theta)} \tag{3}$$

In this paper, different stages of the antenna are discussed to observe the variation of resonant frequency and iteration. Further, the effect of aspect ratio and fractal dimension of the boundary on the performance of the circularly polarized microstrip antenna is presented.

## 2. ANTENNA GEOMETRY AND DESIGN

The generation of stage-1 of the proposed antenna is shown in Fig. 1. The proposed antenna is obtained by replacing each pair of opposite sides of the patch with 1st iterated Koch curve having different indentation angles. This ensures the generation of two orthogonal modes which are closer to each other. The antenna is fed along the diagonal at a suitable position where the impedance of the patch is 50 ohms as indicated in Fig. 2(a). Five different cases have been considered for stage 1, and the geometries of the antenna are illustrated in Fig. 2(b).

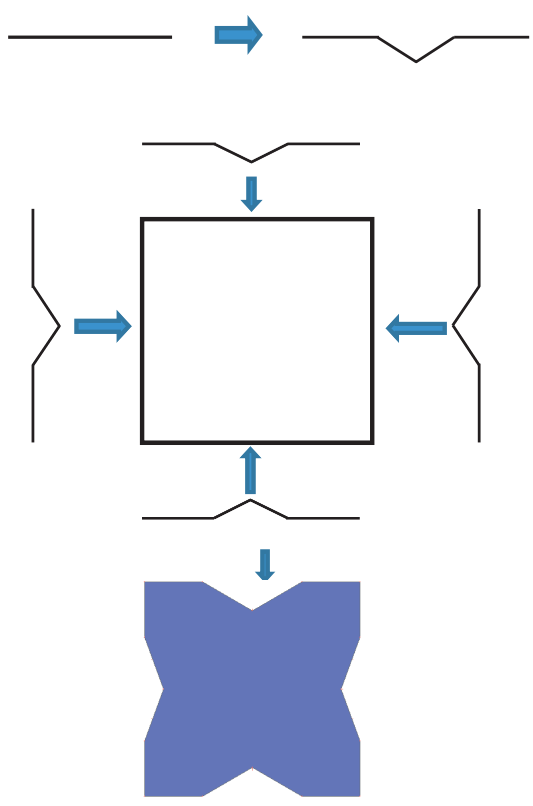

**Figure 1.** Generation of Koch fractal boundary CP antenna stage-1.

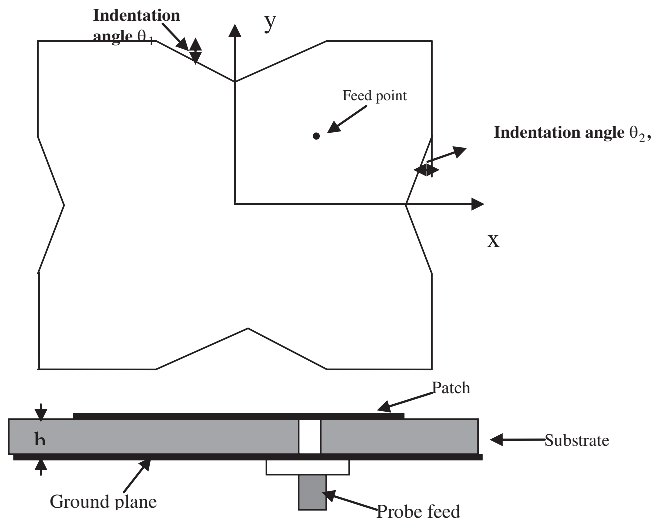


(a)

(b)

**Figure 2.** (a) Feed structure for Koch fractal boundary CP antenna. (b) Geometry of Koch CP antenna stage-1. (i) 13°–0°, (ii) 30°–20°, (iii) 40°–31°, (iv) 50°–43°, (v) 60°–55°.

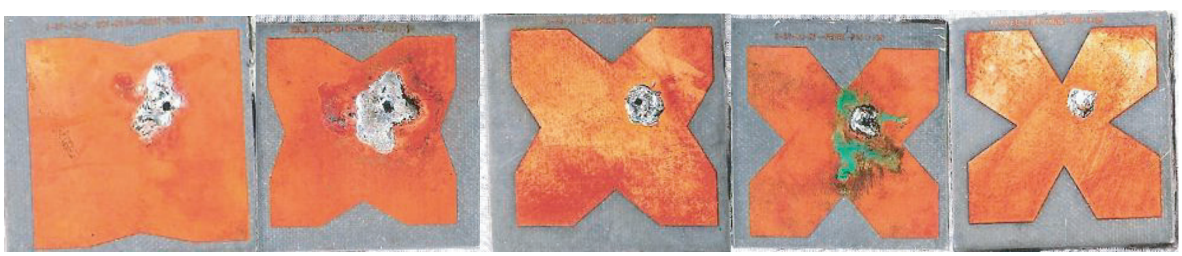

(a) (b) (c) (d) (e)

**Figure 3.** Photographs of fabricated Koch fractal boundary CP antennas stage-1. (a) Koch CP antenna 1. (b) Koch CP antenna 2. (c) Koch CP antenna 3. (d) Koch CP antenna 4. (e) Koch CP antenna 5. Koch CP antenna 1: 13°–0°; Koch CP antenna 2: 30°–20°, Koch CP antenna 3: 40°–31°, **Koch CP antenna** 4: 50°–43°, Koch CP antenna 5: 60°–55°.

All the five antennas are fabricated on RT Duroid substrate of thickness 3.2 mm, relative permittivity of 2.33 and loss tangent of 0.0018. The end to end dimension of the patch is 36.4 mm. Photographs of the fabricated antennas are shown in Fig. 3. Measurements are carried out at Defence Lab, Hyderabad using standard equipment made by Agilent. The rotating linear pattern is measured to verify the axial ratio at the center frequency in the boresight direction. Return loss ($S_{11}$) characteristics are measured to compute impedance bandwidth. Further, the input impedance plotted on Smith chart makes the designer know the center frequency having minimum axial ratio, and the antenna input impedance at the feed point is also shown. The same procedure is followed even for designing 2nd stage Koch CP antenna.

## 3. RESULTS AND DISCUSSION

### 3.1. Koch CP Antenna Stage-1

In order to study the behavior of the proposed antenna, Koch curves of stage 1 and stage 2 are used as boundary to the rectangular microstrip antennas. The simulated $S_{11}$ and axial ratio characteristics of the Koch CP antennas for various cases are shown in Figs. 4 and 5. By observing the graphs it is clear that both the return loss and axial ratio characteristics are shifted towards the origin as indentation angle is increased. All the antennas provide good circular polarization at the center frequency with axial ratio close to 0 dB in the boresight direction. Figs. 6 and 7 show the measured return loss and input impedance of Koch CP antenna-1 operating at 2510 MHz. The frequency corresponding to minimum axial ratio and the tip of the curve in the Smith chart are exactly the same. This indicates that the antenna provides perfect circular polarization at a frequency where the antenna is matched to the line. Fig. 8 shows the radiation pattern measured at 2510 MHz in two orthogonal planes. Fig. 9 depicts the rotating linear pattern for the same antenna which displays the axial ratio in all the directions. The width of the curve in a particular direction gives the axial ratio in that direction. It is clearly seen that this ratio in the boresight direction is almost 0 dB. The simulated and measured $S_{11}$ characteristics of cp antenna stage-1 are shown in Fig. 10.

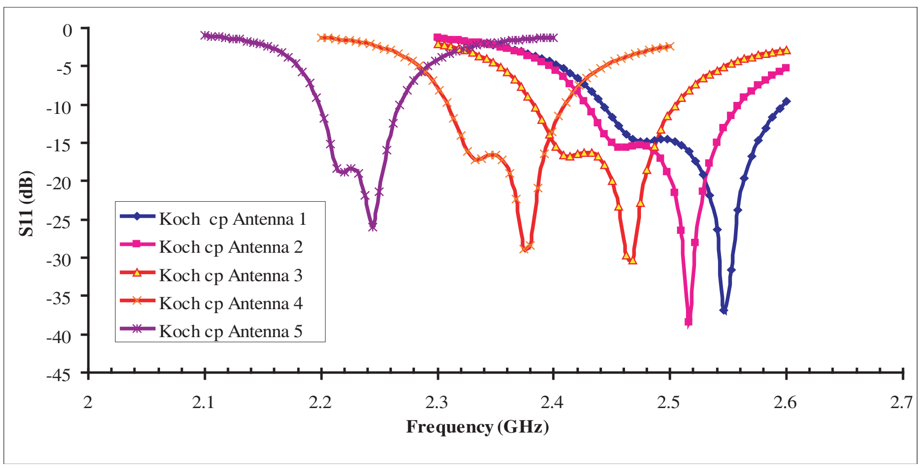


**Figure 4.** $S_{11}$ characteristics of Koch fractal boundary CP antenna stage-1 for different indentation angles.

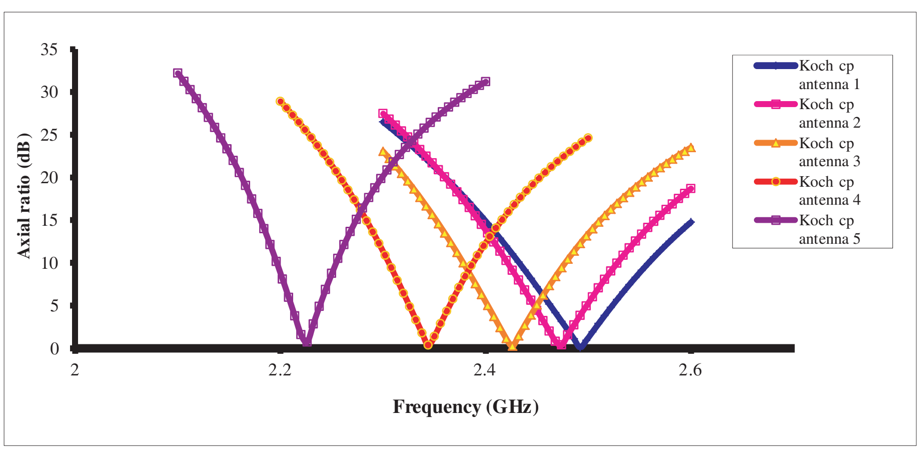


**Figure 5.** Axial ratio vs frequency of Koch fractal boundary cp antenna stage-1 for different indentation angles.

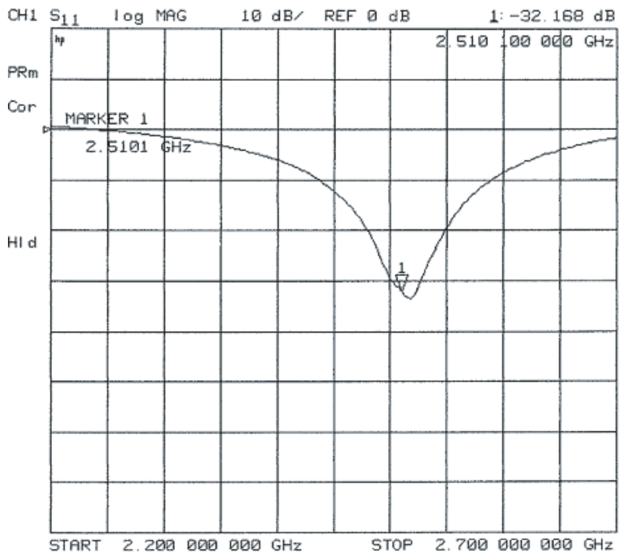


Figure 6. Measured $S_{11}$ characteristics of Koch CP antenna stage-1.

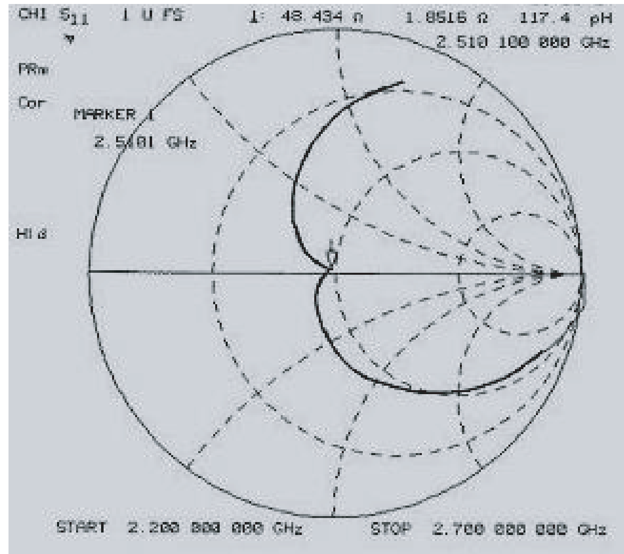


Figure 7. Measured input impedance of Koch CP antenna stage-1.

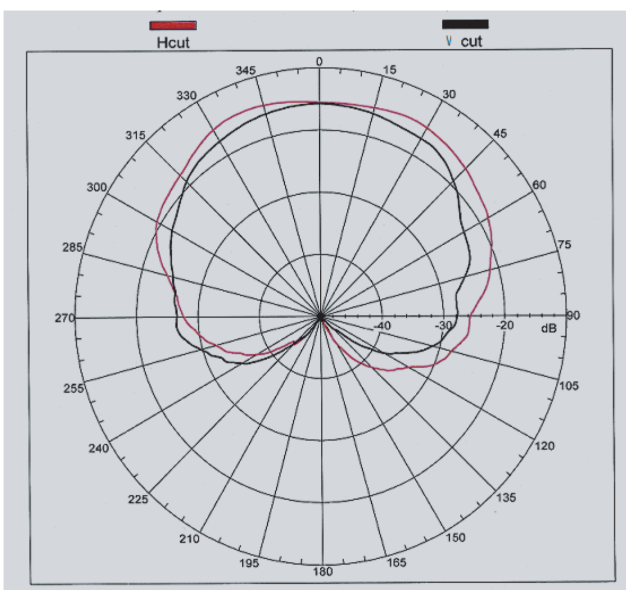


Figure 8. Measured radaition pattern of Koch CP antenna stage 1 in two orthogonal planes at 2510 MHz.

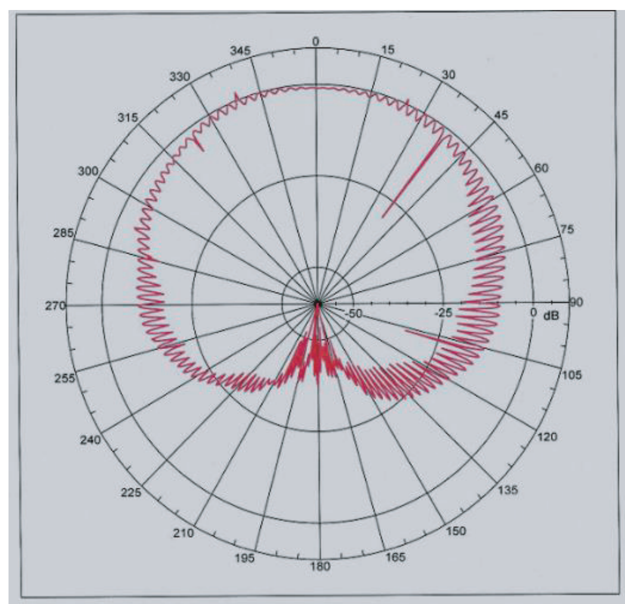

Figure 9. Measured Rotating linear pattern of Koch CP antenna stage 1 at 2510 MHz.

There are different ways through which the eccentricity of circularly polarized antennas can be verified. The first one is with the help of return loss characteristics where the curve contains two close dips corresponding two orthogonal modes. This can be seen from Fig. 4. The second one is through axial ratio characteristics shown in Fig. 5. The AR characteristic shows that the 3 dB axial ratio bandwidth is around 1.6% and with 3 dB axial ratio at the center frequency very close to unity. The third one is through input impedance variation with frequency as shown in Fig. 7. The curve contains a single loop of zero area. The fourth one is through radiation pattern or rotating linear pattern whose width in the boresight direction gives the value of axial ratio. The details of all the antennas are listed in Table 1.

**Table 1.** Summary of results of Koch fractal boundary CP antennas of stage-1.

| **Antenna** | **$\theta$ in $x$ and $y$ direction (deg)** | **Fractal dimension of the boundary** | | **Center frequency (MHz)** | **10 dB impedance Bandwidth (%)** | **3 dB axial ratio bandwidth (%)** |
|---|---|---|---|---|---|---|
| | | **Along $x$ direction** | **Along $y$ direction** | | | |
| Koch CP antenna 1 Stage 1 | 13, 0 | 1.0045 | 1.0000 | 2510 | 6.2 | 1.6 |
| Koch CP antenna 2 Stage 1 | 30, 20 | 1.0526 | 1.0225 | 2472 | 5.25 | 1.3 |
| Koch CP antenna 3 Stage 1 | 40, 31 | 1.0985 | 1.0564 | 2426 | 4.98 | 1.2 |
| Koch CP antenna 4 Stage 1 | 50, 43 | 1.1650 | 1.1160 | 2343 | 4.26 | 1 |
| Koch CP antenna 5 Stage 1 | 60, 55 | 1.2610 | 1.2090 | 2234 | 3 | 0.8 |

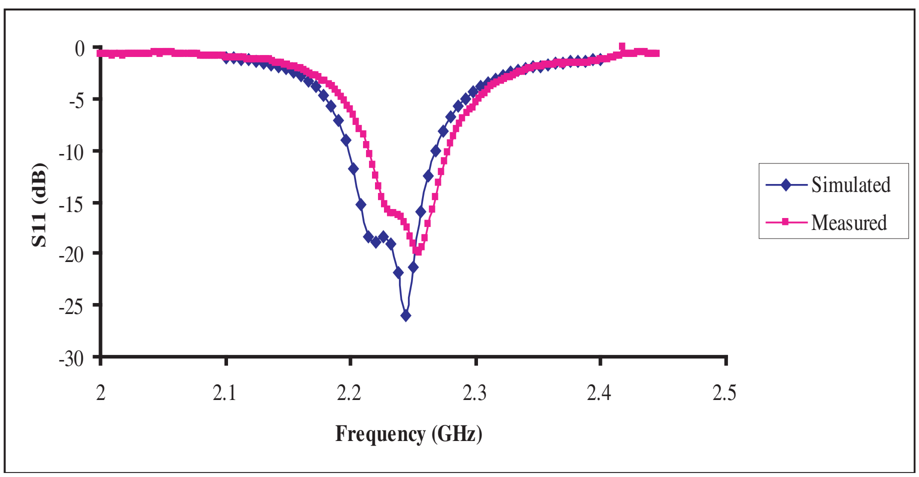


**Figure 10.** $S_{11}$ characteristics of Koch CP antenna-3 of stage-1 simulated and measured.

The results of Koch CP antenna of stage 1 for all the cases are summarized in Table 1. It can be observed that the center frequency of the antenna has been reduced from 2510 MHz to 2234 MHz when indentation angle is changed from 13° to 60° for the first iterated Koch CP antenna. As the indentation angle is changed, the corresponding fractal dimension of the curve also changes accordingly, which is an indication of space filling property of the curve. Hence the fractal dimension of the boundary and resonant frequency at which the antenna resonates giving circular polarization are inversely proportional to each other. It can also be related to aspect ratio which is described in the next section.

### 3.2. Koch CP Antenna Stage-2

The principle enumerated in the previous section to get circular polarization using Koch curve as boundary is also extended to the 2nd stage. Five different cases have been considered here. The geometry of the antennas with different indentation angles are shown in Fig. 11 obviously. When the 2nd stage is used, the electrical length or the perimeter of the patch is increased which lowers the resonant frequency. It is noted that the end to end dimension of the patch remains constant for all the cases. The real estate of the patch is also drastically reduced for higher indentation angles. $S_{11}$ and axial ratio characteristics of the 2nd stage CP antennas for all the cases considered are shown in Figs. 12 and 13, respectively. The details of center frequency, impedance bandwidth, axial ratio bandwidth, etc. of the antenna are listed in Table 2.

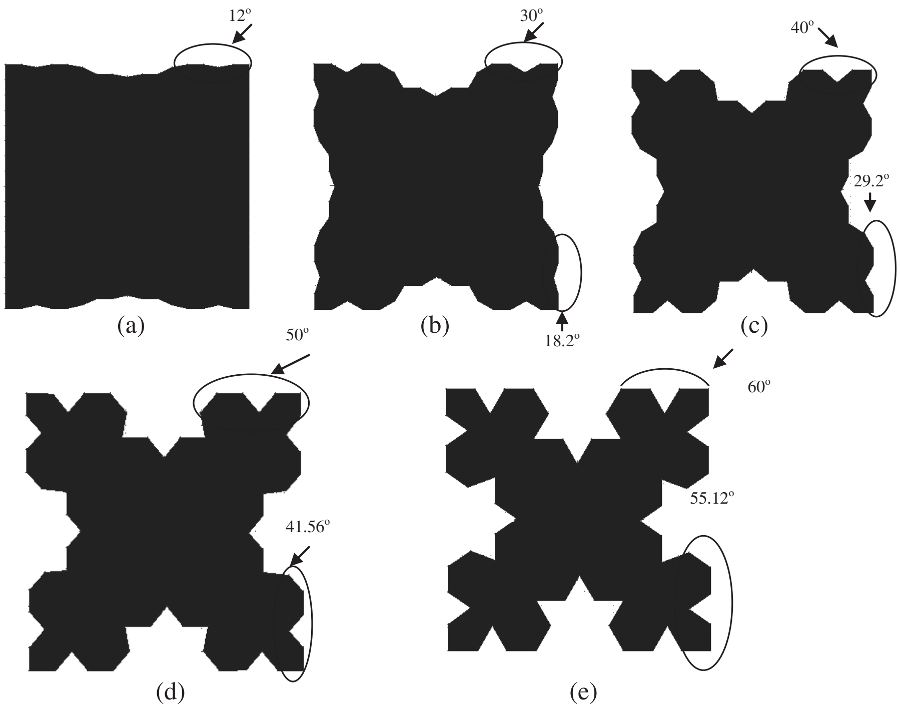


**Figure 11.** Antenna geometry for various cases of 2nd stage Koch fractal boundary CP antennas. (a) Antenna 1: Indentation angle of the boundary along $x$ direction 12° and $y$ direction 0°. (b) Antenna 2: Indentation angle of the boundary along $x$ direction 30° and $y$ direction 18.2°. (c) Antenna 3: Indentation angle of the boundary along $x$ direction 40° and $y$ direction 29.2°. (d) Antenna 4: Indentation angle of the boundary along $x$ direction 50° and $y$ direction 41.56°. (e) Antenna 5: Indentation angle of the boundary along $x$ direction 60° and $y$ direction 55.12°.

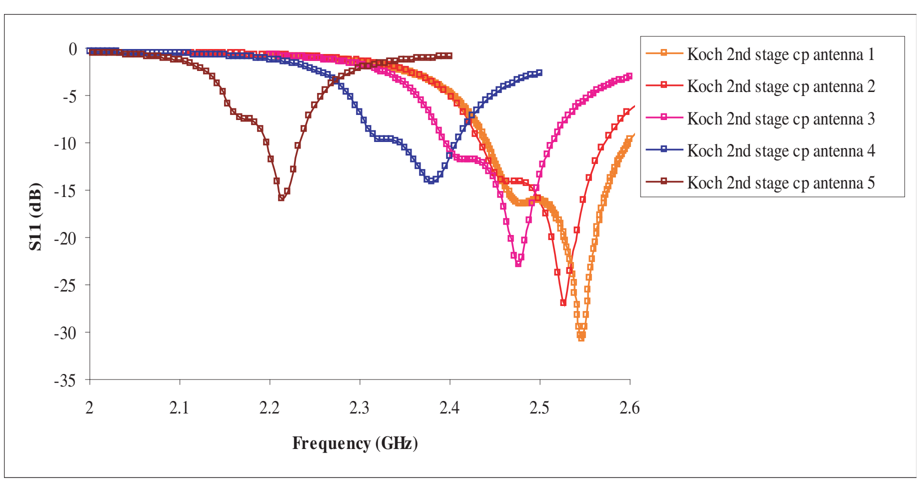


**Figure 12.** $S_{11}$ characteristics of Koch CP 2nd stage CP antenna for different indentation angles.

**Table 2.** Summary of results of Koch fractal boundary CP antenna stage-2.

| Antenna | $\theta$ in $x$ and $y$ directions (deg) | Fractal dimension of the boundary | | Center frequency (MHz) | 10 dB impedance Bandwidth (%) | 3 dB axial ratio bandwidth (%) |
|---|---|---|---|---|---|---|
| | | Along $x$ direction | Along $y$ direction | | | |
| Koch CP antenna 1 stage 2 | 12, 0 | 1.0078 | 1.0000 | 2495 | 6.3 | 1.48 |
| Koch CP antenna 2 Stage 2 | 30, 18.3 | 1.0526 | 1.0187 | 2474 | 5.71 | 1.33 |
| Koch CP antenna 3 Stage 2 | 40, 29.2 | 1.0985 | 1.0496 | 2420 | 4.95 | 1.15 |
| Koch CP antenna 4 Stage 2 | 50, 41.56 | 1.1650 | 1.1073 | 2326 | 4.17 | 0.9 |
| Koch CP antenna 5 Stage 2 | 60, 55.12 | 1.2610 | 1.21 | 2170 | 1.75 | 0.73 |

**Table 3.** Details of aspect ratio and resonant frequency of Koch CP antenna of first stage.

| Antenna | Along $x$ direction | | Along $y$ direction | | Aspect ratio | $f_o$ (MHz) |
|---|---|---|---|---|---|---|
| | $\theta_1$ (deg) | $b$ (mm) | $\theta_2$ (deg) | $a$ (mm) | b/a | |
| Antenna-1 | 13 | 36.872 | 0 | 36.4 | 1.0129 | 2510 |
| Antenna-2 | 30 | 39.013 | 20 | 37.531 | 1.0394 | 2472 |
| Antenna-3 | 40 | 41.22 | 31 | 39.199 | 1.0515 | 2426 |
| Antenna-4 | 50 | 44.31 | 43 | 42.048 | 1.0537 | 2343 |
| Antenna-5 | 60 | 48.533 | 55 | 46.264 | 1.049 | 2234 |

From Table 2 it is inferred that for the 2nd iterated one the $f_o$ is lowered from 2495 MHz to 2170 MHz when the indentation angle of the Koch curve is changed from 12° to 60°. It is observed that the percentage reduction in resonant frequency for the 1st stage is 11%, as it is 13% for the 2nd stage. CP can be obtained only under certain favorable conditions, i.e., when the dimension of the patch satisfies the requirements necessary for generating the two modes as already discussed. This is verified through the aspect ratio (b/a) which can be calculated by computing the length in two perpendicular directions of the patch using the relations given in Eqs. (4) and (5).

$$\left.\begin{aligned} b &= L\left(\frac{4}{2(1+\cos\theta_1)}\right)^n \\ a &= L\left(\frac{4}{2(1+\cos\theta_2)}\right)^n \end{aligned}\right\} \begin{aligned} n &= 1 \text{ for the first iteration} \quad (4) \\ &= 2 \text{ for the 2nd iteration} \quad (5) \end{aligned}$$

where $L$ = Initial side length of the Patch, $\theta_1$ = Indentation angle along $x$-direction, $\theta_2$ = Indentation angle along $y$-direction.

The circular polarization is possible only when the aspect ratio of the patch is within certain limits. For the case of Koch fractal boundary CP antenna stage-1, the ratio should lie between 1.012 and 1.0537 as listed in Table 3. Similarly for the 2nd stage Koch CP antenna the ratio must be within 1.0219 and 1.132 as given in Table 4. Outside this range of aspect ratio, the CP operation is not possible. This

**Table 4.** Details of aspect ratio and resonant frequency of Koch CP antenna of second stage.

| Antenna | Along $x$ direction | | Along $y$ direction | | Aspect ratio | $f_o$ (MHz) |
|---|---|---|---|---|---|---|
| | $\theta_1$ (deg) | $b$ (mm) | $\theta_2$ (deg) | $a$ (mm) | b/a | |
| Antenna-1 | 12 | 37 | 0 | 36.4 | 1.022 | 2495 |
| Antenna-2 | 30 | 41.81 | 18.3 | 38.31 | 1.091 | 2474 |
| Antenna-3 | 40 | 46.68 | 29.2 | 41.5 | 1.124 | 2420 |
| Antenna-4 | 50 | 53.95 | 41.56 | 47.63 | 1.132 | 2326 |
| Antenna-5 | 60 | 64.71 | 55.12 | 58.9 | 1.098 | 2170 |

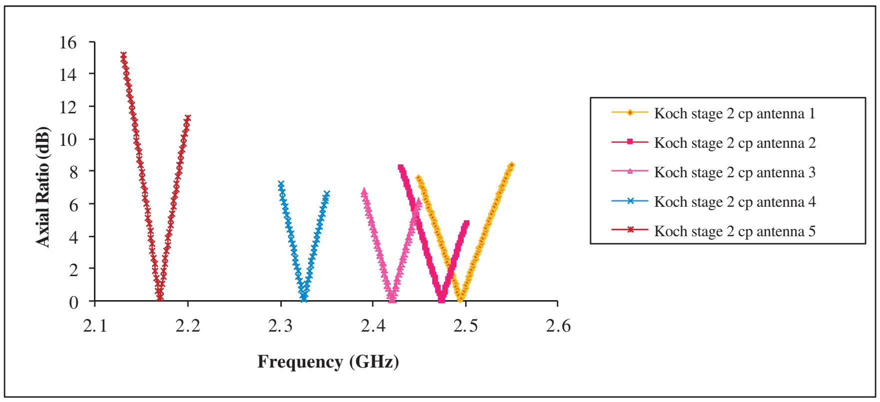


**Figure 13.** Axial ratio characteristics of Koch stage 2 CP antenna for different indention angles.

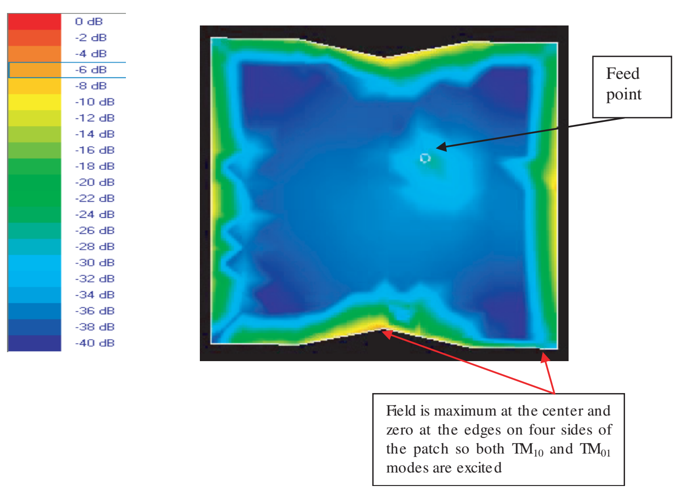


**Figure 14.** Current distribution over the patch with $TM_{10}$ and $TM_{01}$ modes excitation.

range is true only for this substrate. If substrate properties are changed, the range of aspect ratio to get CP may be different [17].

The current distribution over the patch is shown in Fig. 14 which will give an indication of excitation of two modes $TM_{10}$ and $TM_{01}$. On both opposite pairs of the patch it is observed that the current is maximum at the center and zero or minimum at the edges. This is an indication of excitation of $TM_{10}$ or $TM_{01}$ modes, and is the prime requisite to get circular polarization. In order to get circular polarization, two orthogonal modes are excited. Two modes are excited as the patch is fed along the diagonal, and the electrical length in the two opposite pairs is slightly different. This method of obtaining circular polarization is simple compared to the methods presented earlier in the literature. The actual surface area of the patch (real estate) of Koch CP antenna-5 of second stage is 964 $mm^2$ operating at 2170 MHz. If conventional Euclidian shaped nearly square patch is used, it would require approximately 1760 $mm^2$ operating at the same frequency. By observing the graphs and Tables 1 and 2, it is clearly understood that the aspect ratio impacts on the circular polarization.

## 4. CONCLUSION

The proposed Koch fractal boundary CP antenna is compact in size, provides good polarization purity, and is easy to tune the antenna structure for obtaining CP. Further, the antenna operates over a 3 dB AR bandwidth of 40 MHz (1.6%) and 10 dB impedance bandwidth of 155 MHz (6.2%) with center frequency of 2510 MHz. The antenna exhibits a gain of 4 dBi to 6 dBi over the entire band of operation. The aspect ratio and fractal dimension of the boundary play an important role in designing circularly polarized Microstrip antennas. It has been established that the aspect ratio can be varied with fractal dimension of the boundary which will affect the performance of the circularly polarized antenna to get axial ratio close to one.

## REFERENCES


1. Lee, K. F. and W. Chen, *Advances in Microstrip and Printed Antennas*, John Wiley and Sons, New York, 1997.
2. Langston, W. L. and D. R. Jackson, "Impedance, axial ratio and receive power bandwidth of microstrip antennas," *IEEE Transactions on Antennas and Propagation*, Vol. 52, No. 10, 2769–2773, Oct. 2004.
3. Sharma, P. C. and K. C. Gupta, "Analysis and optimized design of single feed circularly polarized microstrip antennas," *IEEE Transactions on Antennas and Propagation*, Vol. 31, 949–955, Nov. 1983.
4. Iwasaki, Hisao., "A circularly polarized small size microstrip antenna with a cross slot," *IEEE Transactions on Antennas and Propagation*, Vol. 44, No. 10, 1399–1401, Oct. 1996.
5. Lee, C. S., V. Nalbandian, and F. Schwering, "Circularly polarized microstrip antenna with a single feed," *IEEE Transactions on Antennas and Propagation*, Vol. 44, No. 10, 1426-27, Oct. 1996.
6. Wong, K. L. and J. Y. Wu, "Single feed small circularly polarized square microstrip antenna," *Electronics Letters*, Vol. 33, No. 22, 1833–1834, Oct. 1997.
7. Chen, W.-S., C.-K. Wu, and K.-L. Wong, "Single feed square ring microstrip antenna with truncated corners for compact circular polarization operation," *Electronic Letters*, Vol. 34, No. 11, 1045–1047, May 1998.
8. Lee, C. S. and V. Nalbandian, "Planar circularly polarized microstrip antenna with a single feed," *IEEE Transactions on Antennas and propagation*, Vol. 47, No. 6, 1005–1007, Jun. 1999.
9. Chen, W. S., "Small circularly polarized microstrip antennas," *IEEE International Antennas and Propagation Society Symposium*, Vol. 1, 256–259, Orlando, FL, USA, 1999.
10. Chen, W.-S., C.-K. Wu, and K. L. Wong, "Novel compact circularly polarized square microstrip antenna," *IEEE Transactions on Antennas and Propagation*, Vol. 49, No. 3, 340–342, Mar. 2001.
11. Yang, K.-P. and K.-L. Wong, "Dual band circularly polarized square microstrip antenna," *IEEE Transactions on Antennas and Propagations*, Vol. 49, No. 3, 377–382, Mar. 2001.
12. Elsdon, M., A. Sambell, S. C. Gao, and Y. Qin, "Compact Circular polarized patch antenna with relaxed manufacturing tolerance and improved axial ratio bandwidth," *Electronics Letters*, Vol. 39, No. 18, 1296–1298, Sep. 2003.
13. Row, J. S. and C. Y. Ai, "Compact design of single feed circularly polarized microstrip antenna," *Electronics Letters*, Vol. 4, No. 18, 1093–1094, Sep. 2004.
14. Wong, M. L., H. Wong, and K. M. Luk, "Small circularly polarized patch antenna," *Electronics Letters*, Vol. 41, No. 16, 7–8, Aug. 2005.

15. Rao, P. N. and P. R. Yagateela, "Compact singe feed circularly polarized Koch island microstrip antenna," *International Journal of Electronics and Communications*, Vol. 70, 2016, 1543–1550, Elsevier Publications, Sep. 2016.
16. Sharma, P. C. and K. C. Gupta, "Analysis and optimized design of singe feed circularly polarized microstrip antennas," *IEEE Transactions on Antennas and Propagation*, Vol. 31, 949–955, Nov. 1983.
17. Vinoy, K. J., J. K. Abraham, and V. K. Vardan, "On the relationship between Fractal dimension and the performance of multi-resonant dipole antennas using Koch curves," *IEEE Transactions on Antennas and Propagation*, Vol. 51, No. 9, 2296–2303, Sep. 2003.
18. Farswan, A., A. K. Gautam, B. K. Kanaujia, and K. Rambabu, "Design of Koch fractal circularly polarized antenna for handheld UHF RFID reader applications," *IEEE Transactions on Antennas and Propagation*, Vol. 64, No. 2, 771–775, 2016, DOI 10.1109/TAP.2015.2505001.